



**HAL**  
open science

## **Culture and identification of a “Deltamicon” SARS-CoV-2 in a three cases cluster in southern France**

Philippe Colson, Pierre-edouard Fournier, Jeremy Delerce, Matthieu Million,  
Marielle Bedotto, Linda Houhamdi, Nouara Yahy, Jeremy Bayette, Anthony  
Levasseur, Jacques Fantini, et al.

### ► **To cite this version:**

Philippe Colson, Pierre-edouard Fournier, Jeremy Delerce, Matthieu Million, Marielle Bedotto, et al..  
Culture and identification of a “Deltamicon” SARS-CoV-2 in a three cases cluster in southern France.  
2024. hal-03678601

**HAL Id: hal-03678601**

**<https://amu.hal.science/hal-03678601>**

Preprint submitted on 7 Feb 2024

**HAL** is a multi-disciplinary open access archive for the deposit and dissemination of scientific research documents, whether they are published or not. The documents may come from teaching and research institutions in France or abroad, or from public or private research centers.

L'archive ouverte pluridisciplinaire **HAL**, est destinée au dépôt et à la diffusion de documents scientifiques de niveau recherche, publiés ou non, émanant des établissements d'enseignement et de recherche français ou étrangers, des laboratoires publics ou privés.

1 **TITLE PAGE**

2

3 **Type of article: Research article**

4

5 **Full-length title:**

6 **Culture and identification of a “Deltamicon” SARS-CoV-2 in a three cases cluster in**

7 **southern France**

8

9 **Short title (for the running head): Emergence of a SARS-CoV-2 Delta/Omicron**

10 **recombinant**

11

12 **Author list: Philippe COLSON<sup>1,2,3</sup> \*, Pierre-Edouard FOURNIER<sup>1,2,4</sup>, Jeremy**

13 **DELERCE<sup>1</sup>, Matthieu MILLION<sup>1,2,3</sup>, Marielle BEDOTTO<sup>1</sup>, Linda HOUHAMDI<sup>1</sup>,**

14 **Nouara YAHY<sup>5</sup>, Jeremy BAYETTE<sup>6</sup>, Anthony LEVASSEUR<sup>1,2</sup>, Jacques FANTINI<sup>5</sup>,**

15 **Didier RAOULT<sup>1,2</sup>, Bernard LA SCOLA<sup>1,2,3</sup> \***

16 **Affiliations:** <sup>1</sup> IHU Méditerranée Infection, 19-21 boulevard Jean Moulin, 13005 Marseille,

17 France; <sup>2</sup> Aix-Marseille Univ., Institut de Recherche pour le Développement (IRD), Microbes

18 Evolution Phylogeny and Infections (MEPHI), 27 boulevard Jean Moulin, 13005 Marseille,

19 France; <sup>3</sup> Assistance Publique-Hôpitaux de Marseille (AP-HM), 264 rue Saint-Pierre, 13005

20 Marseille, France; <sup>4</sup> Aix-Marseille Univ., Institut de Recherche pour le Développement (IRD),

21 Vecteurs – Infections Tropicales et Méditerranéennes (VITROME), 27 boulevard Jean

22 Moulin, 13005 Marseille, France; <sup>5</sup> Aix-Marseille Université, INSERM UMR S 1072, 51

23 boulevard Pierre Dramard, 13015 Marseille, France; <sup>6</sup> LBM Inovie Labosud, 90 rue Nicolas

24 Chedville, 34070, Montpellier, France.

25 **\* Corresponding author:** Bernard La Scola, IHU Méditerranée Infection, 19-21 boulevard

**NOTE: This preprint reports new research that has not been certified by peer review and should not be used to guide clinical practice.**

26 Jean Moulin, 13005 Marseille, France. Tel.: +33 413 732 401, Fax: +33 413 732 402; email:

27 [bernard.la-scola@univ-amu.fr](mailto:bernard.la-scola@univ-amu.fr); Philippe Colson, IHU Méditerranée Infection, 19-21

28 boulevard Jean Moulin, 13005 Marseille, France. Tel.: +33 413 732 401, Fax: +33 413 732

29 402; email: [philippe.colson@univ-amu.fr](mailto:philippe.colson@univ-amu.fr)

30 **Key words:** SARS-CoV-2; recombinant; variant; lineage; Delta; Omicron; Deltamicron;

31 epidemic

32 **Word counts:** abstract, 180; text, 2,364

33 **Figures:** 3; **Table:** 1; **References:** 47

34

35

36  
37  
38  
39  
40  
41  
42  
43  
44  
45  
46  
47  
48  
49  
50  
51  
52  
53  
54

## ABSTRACT

Multiple SARS-CoV-2 variants have successively, or concomitantly spread worldwide since summer 2020. A few co-infections with different variants were reported and genetic recombinations, common among coronaviruses, were reported or suspected based on co-detection of signature mutations of different variants in a given genome. Here we report three infections in southern France with a Delta 21J/AY.4-Omicron 21K/BA.1 “Deltamicron” recombinant. The hybrid genome harbors signature mutations of the two lineages, supported by a mean sequencing depth of 1,163-1,421 reads and mean nucleotide diversity of 0.1-0.6%. It is composed of the near full-length spike gene (from codons 156-179) of an Omicron 21K/BA.1 variant in a Delta 21J/AY.4 lineage backbone. Importantly, we cultured an isolate of this recombinant and sequenced its genome. It was observed by scanning electron microscopy. As it is misidentified with current variant screening qPCR, we designed and implemented for routine diagnosis a specific duplex qPCR. Finally, structural analysis of the recombinant spike suggested its hybrid content could optimize viral binding to the host cell membrane. These findings prompt further studies of the virological, epidemiological, and clinical features of this recombinant.

55

## TEXT

56

### 57 **Introduction**

58         The current SARS-CoV-2 pandemic has highlighted since the summer of 2020 the  
59 successive or concomittant emergence of numerous viral variants, each causing a specific  
60 epidemic.<sup>1-3</sup> Some of these variants spread to become pandemic while others remained  
61 epidemic in a restricted geographical area. The variants characterized so far have been shaped  
62 by nucleotide substitutions, insertions or deletions. However, another major evolutionary  
63 mechanism of RNA viruses is genetic recombination, which is very common among  
64 coronaviruses.<sup>4-8</sup> It requires co-infection of the same host cell by two viruses, which may be  
65 two distinct mutants or variants.<sup>9</sup> Therefore, the frequency of creation of recombinants  
66 between two variants depends on the duration of their co-circulation, on the time until viral  
67 clearance, and on the number of people exposed to both viruses. Co-infections with two  
68 variants were reported including recently with SARS-CoV-2 Delta and Omicron variants.<sup>10-13</sup>  
69 Furthermore, genetic recombinations were reported or suspected, based on the concurrent  
70 detection in consensus genomes of signature mutations of different mutants or variants.<sup>10,12,14-</sup>  
71 <sup>24</sup> A study detected up to 1,175 (0.2%) putative recombinant genomes among 537,360  
72 genomes and estimated that up to 5% SARS-CoV-2 having circulated in the USA and UK  
73 could be recombinants.<sup>16</sup>

74         Two pandemic variants, Delta and Omicron 21K (Nextclade classification<sup>25,26</sup>)/BA.1  
75 (Pangolin classification<sup>27</sup>), recently succeeded each other as the predominant viruses but co-  
76 circulated for a period of several weeks, creating conditions for co-infections and  
77 subsequently recombinations. This period spanned between December 27<sup>th</sup>, 2021 and  
78 February 14<sup>th</sup>, 2022 in our geographical area, as assessed by our SARS-CoV-2 genotypic  
79 surveillance based on variant-specific qPCR and next-generation genomic sequencing.<sup>3,28,29</sup> In

80 January 2022, genomes harboring mutations from both Delta and Omicron 21K/BA.1 variants  
81 were reported in Cyprus but it was questioned whether sequences might have resulted from  
82 contamination.<sup>23</sup> Still, 15 genomes as of 27/02/2022 being hybrids of these two variants and  
83 highly similar between each other were reported since February 2022 ([https://github.com/cov-  
84 lineages/pango-designation/issues/444](https://github.com/cov-lineages/pango-designation/issues/444)). We herein report three infections by a recombinant  
85 SARS-CoV-2 Delta 21K/AY.4-Omicron 21K/BA.1 whose genome is highly similar to the 15  
86 previously reported genomes and the isolation of the recombinant virus from one of the  
87 patients.

88

## 89 **Materials and methods**

90 Nasopharyngeal samples were collected from two patients in our university hospital  
91 institute (Méditerranée Infection; <https://www.mediterranee-infection.com/>) and tested for  
92 SARS-CoV-2 infection by real-time reverse transcription-PCR (qPCR) as previously  
93 described.<sup>3,28,29</sup> The third patient was sampled in a private medical biology laboratory in  
94 southern France (Inovie Labosud, Montpellier, France). qPCR assays that screen for SARS-  
95 CoV-2 variants were performed as recommended by French public health authorities  
96 ([https://www.data.gouv.fr/fr/datasets/donnees-de-laboratoires-pour-le-depistage-indicateurs-  
97 sur-les-mutations/](https://www.data.gouv.fr/fr/datasets/donnees-de-laboratoires-pour-le-depistage-indicateurs-sur-les-mutations/)). In our center this included the detection of spike mutation among which  
98 K417N (Thermo Fisher Scientific, Waltham, USA), combined with testing with the TaqPath  
99 COVID-19 kit (Thermo Fisher Scientific) that target viral genes ORF1, N (nucleocapsid) and  
100 S (spike), as previously reported.<sup>3,28,29</sup> The private medical laboratory used the ID SARS-  
101 CoV-2/VOC Revolution Pentaplex assay (ID Solutions, Grabels, France) that detects spike  
102 mutations K417N, L452R, and E484K (Pentaplex assay, ID Solution, France).

103 SARS-CoV-2 genomes were sequenced in the framework of genomic surveillance  
104 implemented since February 2020<sup>3</sup> in our institute. Next-generation sequencing was

105 performed with the Illumina COVID-seq protocol on the NovaSeq 6000 instrument (Illumina  
106 Inc., San Diego, CA, USA) or with the Oxford Nanopore technology (ONT) on a GridION  
107 instrument (Oxford Nanopore Technologies Ltd., Oxford, UK) combined with prior multiplex  
108 PCR amplification according to the ARTIC procedure (<https://artic.network/>), as previously  
109 described,<sup>3,28</sup> with the ARTIC nCoV-2019 Amplicon Panel v4.1 of primers (IDT, Coralville,  
110 IA, USA). Then, sequence read processing and genome analysis were performed as  
111 previously described.<sup>3,28</sup> Briefly, for Illumina NovaSeq reads, base calling was performed  
112 with the Dragen Bcl Convert pipeline [v3.9.3;  
113 [https://emea.support.illumina.com/sequencing/sequencing\\_software/bcl-convert.html](https://emea.support.illumina.com/sequencing/sequencing_software/bcl-convert.html)  
114 (Illumina Inc.)], mapping was performed with the bwa-mem2 tool (v. 2.2.1;  
115 <https://github.com/bwa-mem2/bwa-mem2>) on the Wuhan-Hu-1 isolate genome (GenBank  
116 accession no. NC\_045512.2) then cleaned with Samtools (v. 1.13; <https://www.htslib.org/>),  
117 variant calling was carried out with freebayes (v. 1.3.5;  
118 <https://github.com/freebayes/freebayes>) and consensus genomes were built using Bcftools (v.  
119 1.13; <https://samtools.github.io/bcftools/bcftools.html>). ONT reads were processed with the  
120 ARTIC-nCoV-bioinformaticsSOP pipeline v1.1.0 ([https://github.com/artic-  
121 network/fieldbioinformatics](https://github.com/artic-)). Nucleotide and amino acid changes relatively to the Wuhan-  
122 Hu-1 isolate genome were obtained using the Nextclade tool  
123 (<https://clades.nextstrain.org/>).<sup>25,26</sup> Nextstrain clades and Pangolin lineages were determined  
124 using the Nextclade web application (<https://clades.nextstrain.org/>)<sup>25,26</sup> and the Pangolin tool  
125 (<https://cov-lineages.org/pangolin.html>),<sup>27</sup> respectively. Genome sequences described here  
126 were deposited in the GenBank sequence database (<https://www.ncbi.nlm.nih.gov/genbank/>)<sup>30</sup>  
127 (OM990851, OM990852, OM991095, OM991295), and on the IHU Méditerranée Infection  
128 website (<https://www.mediterranee-infection.com/sars-cov-2-recombinant/>). The Simplot  
129 software (<https://sray.med.som.jhmi.edu/SCROftware/SimPlot/>)<sup>31</sup> was used for recombination

130 analysis. Phylogeny was reconstructed by the IQTree (v2.1.3; <http://www.iqtree.org/>)<sup>32</sup> or  
131 MEGA X<sup>33</sup> (v10.2.5; <https://www.megasoftware.net/>) tools and visualized with MEGA X  
132 after sequence alignment with MAFFT (<https://mafft.cbrc.jp/alignment/server/>).<sup>34</sup> As  
133 phylogenetic analysis can hardly applies to sequences that have different evolutionary  
134 histories, we built two separate trees, a first one for the regions classified as of the Delta  
135 21J/AY.4 variant (positions 1-22,128 and 25,519-29,903 in reference to the genome of the  
136 Wuhan-Hu-1 isolate), and a second one for the regions classified as of the Omicron 21K/BA.1  
137 variant (positions 22,129-25,519). The 10 genomes the closest genetically to these fragments  
138 of the genome obtained here were selected through a BLAST<sup>35</sup> search among genomes of the  
139 Delta 21J/AY.4 and Omicron 21K/BA.1 variants in the sequence database of our institute that  
140 contains approximately 50,000 SARS-CoV-2 genomes; then, they were incorporated in the  
141 phylogeny together with the genome of the Wuhan-Hu-1 isolate. As a matter of fact, it should  
142 not be acceptable to make a phylogenetic tree based on concatenation of sequences from  
143 different origin.

144 SARS-CoV-2 culture isolation was performed by inoculating 200  $\mu$ L of respiratory  
145 sample on Vero E6 cells as previously described.<sup>36</sup> Cytopathic effect was observed by  
146 inverted microscopy. Viral particles were visualized in the culture supernatant by scanning  
147 electron microscopy with a SU5000 microscope (Hitachi High-Technologies Corporation,  
148 Tokyo, Japan), as previously described.<sup>37</sup>

149 Structural predictions of the spike protein were performed as previously  
150 described.<sup>28,38,39</sup> Briefly, amino acid changes were introduced in the framework of a complete  
151 14-1,200 structure of the original SARS-CoV-2 20B spike and missing amino acids were  
152 incorporated with the Robetta protein structure prediction tool (<https://rosetta.bakerlab.org/>)  
153 before energy minimization through the Polak-Ribière algorithm.

154 A in house duplex qPCR assay specific of the SARS-CoV-2 recombinant was



155 designed that targets the genomes of the Delta 21J [targeted mutation: A11201G in the Nsp6  
156 gene (corresponding to amino acid substitution T77A)] and the Omicron 21K/BA.1 [targeted  
157 mutations: A23040G, G23048A, A23055G in the spike gene (Q493R, G496S, Q498R)]  
158 variants. The sequences of the primers and probes (in 5'-3' orientation) are as follows: (i) for  
159 the Delta 21J-targeting system: forward primer, CTGCTTTTGCAATGATGTTTGT; reverse  
160 primer, TACGCATCACCCAAGTAGCA; probe, 6FAM-  
161 CTTGCCGCTGTAGCTTATTTTAAT (primers and probe concentrations in the mix were  
162 200 nM and 150 nM, respectively); (ii) for the Omicron 21K/BA.1-targeting system: forward  
163 primer, CCTTGTAATGGTGTGAAGGTTTT; reverse primer,  
164 CTGGTGCATGTAGAAGTTCAAAG; probe, 6VIC-  
165 TTTACGATCATATAGTTTCCGACCC (primers and probe concentrations in the mix were  
166 250 nM and 200 nM, respectively).

167 This study was approved by the ethics committee of University Hospital Institute  
168 Méditerranée Infection (No. 2022-001).

169

## 170 **Results**

171 The three case-patients were SARS-CoV-2-diagnosed on nasopharyngeal samples  
172 collected in February 2022. Cycle threshold values (Ct) of diagnostic qPCR were between 20-  
173 21. The patients were below 40 years of age. They resided in southern France and did not  
174 travel abroad recently. They presented mild respiratory symptoms. Two were vaccinated  
175 against SARS-CoV-2 (with two or three doses administered). Variant screening qPCR for the  
176 2 samples collected in our institute showed positivity for the K417N mutation while the  
177 TaqPath COVID-19 kit provided positive signals for all three genes targeted (ORF1, S, and  
178 N). The third sample showed positivity for the K417N mutation and negativity for the L452R  
179 and E484K mutations. Thus, overall, qPCR carried out on the three samples were indicative

180 of a Omicron variant.

181 The three viral genomes [GenBank Accession no. OM990851, OM990852,  
182 OM991095 (<https://www.ncbi.nlm.nih.gov/genbank/>)<sup>30</sup>; available on the IHU Méditerranée  
183 Infection website (<https://www.mediterranee-infection.com/sars-cov-2-recombinant/>)] were  
184 hybrids of Delta 21J/AY.4 and Omicron 21K/BA.1 variant genomes (**Figures 1a, b, c; Table**  
185 **1**). At positions harboring mutations compared to the genome of the Wuhan-Hu-1 isolate,  
186 mean sequencing depth was between 1,163-1,421 reads and mean prevalence of the  
187 majoritary nucleotide was between 99.4-99.9% (with minimum values between 80.3-98.7%),  
188 ruling out the concurrent presence of two variants in the samples either due to co-infection or  
189 to contamination. In this SARS-CoV-2 recombinant, most of the spike gene was replaced in a  
190 Delta 21J/AY.4 matrix by an Omicron 21K/BA.1 sequence (**Figures 1a, b, c**). Indeed, the  
191 recombination sites were located between nucleotide positions 22,034 and 22,194 for the first  
192 one, and between nucleotide positions 25,469 and 25,584 for the second one. These regions  
193 corresponds to amino acids 158 to 211 of the spike protein and to amino acids 26 to 64 of the  
194 ORF3a protein whose gene is contiguous to the spike gene. The Simplot recombination  
195 analysis tool provided congruent results.

196 Genomes from two of the three patients were identical and clustered in the  
197 phylogenetic analysis (**Figures 1d, e**) despite no epidemiological link was documented  
198 between these two patients. The third genome exhibited 5 nucleotide differences.  
199 Phylogenetic analyses showed that most of the recombinant genomes was most closely related  
200 to Delta 21J/AY.4 variant genomes identified in our institute, while the region spanning a  
201 large part of their spike gene was most closely related to Omicron 21K/BA.1 variant genomes  
202 identified in our institute.

203 The respiratory sample from which the first recombinant genome was obtained was  
204 inoculated on Vero E6 cells the day following recombinant identification, and cytopathic

205 effect was observed after 4 days (**Figures 2a, b**; collection of strains of IHU Méditerranée  
206 Infection, no. IHUMI-6070VR). The same day, supernatant was collected and next-generation  
207 genome sequencing was performed using Nanopore technology on a GridION instrument  
208 after PCR amplification with Artic primers, which allowed obtaining the genome sequence of  
209 the viral isolate 8 h later [GenBank Accession no. OM991295  
210 (<https://www.ncbi.nlm.nih.gov/genbank/>)<sup>30</sup>; available on the IHU Méditerranée Infection  
211 website (<https://www.mediterranee-infection.com/sars-cov-2-recombinant/>)]. At mutated  
212 positions compared to the Wuhan-Hu-1 isolate genome, mean sequencing depth was 2,771  
213 reads and mean prevalence of the majoritary nucleotide was 99.1% (minimum, 95.1%), and  
214 the consensus genome was identical to that obtained from the respiratory sample, showing  
215 unambiguously that the virus isolated was the Delta 21J/AY.4-Omicron 21K/BA.1  
216 recombinant. Finally, viral particles were observed in the culture supernatant by scanning  
217 electron microscopy with a SU5000 microscope within minutes after supernatant collection  
218 (**Figure 2c**).

219 The overall structure of the recombinant spike protein was predicted (**Figures 3a-c**).  
220 When superimposed with the spike of the Omicron 21K/BA.1 variant, the main structural  
221 changes were located in the N-terminal domain (NTD). In this region, the surface of the  
222 recombinant spike protein is enlarged, flattened, and more electropositive, a property that is  
223 characteristic of the Delta 21J/AY.4 NTD (**Figure 3c**). In the initial interaction of the virus  
224 with the plasma membrane of the host cells, the NTD is attracted by lipid rafts, which  
225 provides an electronegative landing platforms for the spike.<sup>38,39</sup> Thus, an increase in the  
226 electrostatic surface of the NTD is expected to accelerate the binding of the virus to lipid rafts,  
227 which may confer a selective kinetic advantage against virus competitors.<sup>38</sup> The receptor  
228 binding domain (RBD) of the recombinant is clearly inherited from the Omicron 21K/BA.1  
229 variant (**Figure 3c**). The consequence is also an increase in the electrostatic surface potential

230 of the RBD, which may facilitate the interaction with the electronegative interface of the  
231 ACE-2 cellular receptor. Overall, this structural analysis suggests that the recombinant virus  
232 could have been selected on the basis of kinetic properties conferred by a convergent increase  
233 of the electrostatic potential of both the NTD and the RBD, together with an enlargement of  
234 the NTD surface, all features that suggest an optimization of virus binding to the host cell  
235 membrane.

236 Currently used qPCR screening assays were not able to discriminate this Delta  
237 21J/AY.4-Omicron 21K/BA.1 recombinant and the Omicron 21K/BA.1 variant because the  
238 Delta variant signature mutation detected is absent from the recombinant genome. Therefore,  
239 we attempted to promptly implement a specific qPCR assay that could be used to detect the  
240 recombinant for routine diagnosis use. This was achieved in one day by selecting qPCR  
241 systems from our toolbox of dozens of in house qPCR systems that were designed since the  
242 emergence of the first variant during summer 2020 to specifically target SARS-CoV-2  
243 variants or mutants.<sup>3,40</sup> Two systems that target either the Delta 21J variant or the Omicron  
244 BA.1 variant were combined in a duplex qPCR that can screen for the recombinant. In  
245 preliminary assessment, both tested recombinant-positive samples were positive for the Delta  
246 21J and Omicron BA.1 targets. In addition, 7 Delta non-21J-positive samples were negative  
247 for both targets, 4 Delta 21J-positive samples were positive for the Delta 21J target but  
248 negative for the Omicron BA.1 target, and 3 Omicron BA.1-positive samples were negative  
249 for the Delta 21J target but positive for the Omicron BA.1 target.

250

## 251 **Discussion**

252 It is increasingly demonstrated that the genomes of most biological entities, whatever  
253 their level of complexity, are mosaics of sequences from various origins.<sup>41-45</sup> The present  
254 observations show us in real life the recombination potential of SARS-CoV-2, already largely

255 established for other coronaviruses.<sup>4-6,8,46</sup> and reported or suspected for SARS-CoV-2.<sup>10,12,14-24</sup>  
256 SARS-CoV-2 recombinations were difficult to spot when only genetically very similar  
257 viruses were circulating, as was the case in Europe during the first epidemic episode with  
258 mutants derived from the Wuhan-Hu-1 virus. The increasing genetic diversity of SARS-CoV-  
259 2, the tremendous number of infections at global and national levels, and the unprecedented  
260 global effort of genomic sequencing (<https://covariants.org/per-country>),<sup>3,25,47</sup> raised the  
261 probability of detecting recombinants. Such observations will probably make it possible in the  
262 short or medium term to assess the recombination rate of SARS-CoV-2, whether there are  
263 recombination hotspots, and to what extent recombinations between different variants can  
264 generate new viable, and epidemic variants. This questions on the impact of recombinations  
265 on viral replication and transmissibility, and on clinical severity, as well as on the virus ability  
266 to escape neutralizing antibodies elicited by vaccines or a previous infection. In this view,  
267 culture isolation of SARS-CoV-2 recombinants as was carried out here for the first time to  
268 our knowledge is of primary importance. This variant mentioned recently has no known  
269 epidemic potential. This will allow studying their phenotypic properties, among which their  
270 replicative capacity in various cell lines, their sensitivity to antibodies, or their genetic  
271 evolution *in vitro*. Concurrently, a high level of genomic surveillance must be maintained in  
272 order to detect and characterize all recombination events and circulating recombinants, which  
273 is a critical scientific and public health issue.

274

275

## 276 **Acknowledgments**

277 We are very grateful to Clio Grimaldier, Rita Zgheib, Claudia Andrieu, Ludivine Bréchar,   
278 Raphael Tola, Anthony Fontanini, and Jacques Bou Khalil for their technical help.

## 279 **Author contributions**

280 Study conception and design: Philippe Colson, Pierre-Edouard Fournier, Jacques Fantini,  
281 Didier Raoult, Bernard La Scola. Materials, data and analysis tools: Philippe Colson, Pierre-  
282 Edouard Fournier, Jeremy Delerce, Matthieu Million, Marielle Bedotto, Linda Houhamdi,  
283 Nouara Yahy, Jeremy Bayette, Jacques Fantini. Data analyses: Philippe Colson, Pierre-  
284 Edouard Fournier, Jeremy Delerce, Marielle Bedotto, Anthony Levasseur, Jacques Fantini,  
285 Didier Raoult, Bernard La Scola. Writing of the first draft of the manuscript: Philippe Colson,  
286 Jacques Fantini, and Pierre-Edouard Fournier. All authors read, commented on, and approved  
287 the final manuscript.

### 288 **Funding**

289 This work was supported by the French Government under the “Investments for the Future”  
290 program managed by the National Agency for Research (ANR), Méditerranée-Infection 10-  
291 IAHU-03; by Région Provence Alpes Côte d’Azur and European funding FEDER PRIMMI  
292 (Fonds Européen de Développement Régional-Plateformes de Recherche et d’Innovation  
293 Mutualisées Méditerranée Infection), FEDER PA 0000320 PRIMMI; by Hitachi High-  
294 Technologies Corporation, Tokyo, Japan; and by the French Ministry of Higher Education,  
295 Research and Innovation (ministère de l’Enseignement supérieur, de la Recherche et de  
296 l’Innovation) and the French Ministry of Solidarity and Health (Ministère des Solidarités et de  
297 la Santé).

### 298 **Data availability**

299 The dataset generated during the current study is available from the GenBank database  
300 (<https://www.ncbi.nlm.nih.gov/genbank/>)<sup>30</sup> (GenBank Accession no. OM990851, OM990852,  
301 OM991095, OM991295) and from the IHU Méditerranée Infection website  
302 (<https://www.mediterranee-infection.com/sars-cov-2-recombinant/>).

### 303 **Conflicts of interest**

304 Didier Raoult has a conflict of interest as having been a consultant for Hitachi High-

305 Technologies Corporation, Tokyo, Japan from 2018 to 2020. He is a scientific board member  
306 of Eurofins company and a founder of a microbial culture company (Culture Top). All other  
307 authors have no conflicts of interest to declare. Funding sources had no role in the design and  
308 conduct of the study; collection, management, analysis, and interpretation of the data; and  
309 preparation, review, or approval of the manuscript.

### 310 **Ethics**

311 This study has been approved by the ethics committee of the University Hospital Institute  
312 Méditerranée Infection (No. 2022-001). Access to the patients' biological and registry data  
313 issued from the hospital information system was approved by the data protection committee  
314 of Assistance Publique-Hôpitaux de Marseille (APHM) and was recorded in the European  
315 General Data Protection Regulation registry under number RGPD/APHM 2019-73.

316

317

## REFERENCES

- 318 1. Lemey P, Ruktanonchai N, Hong SL, et al. Untangling introductions and persistence in  
319 COVID-19 resurgence in Europe. *Nature*. 2021;595:713-717.
- 320 2. Hodcroft EB, Zuber M, Nadeau S, et al.. Emergence and spread of a SARS-CoV-2  
321 variant through Europe in the summer of 2020. *Nature*. 2021;595:707-712.
- 322 3. Colson P, Fournier PE, Chaudet H, et al. Analysis of SARS-CoV-2 variants from  
323 24,181 patients exemplifies the role of globalization and zoonosis in pandemics. *Front*  
324 *Microbiol*. 2022b;12:786233.
- 325 4. Lai MMC. Recombination in large RNA viruses: Coronaviruses. *Semin Virol*.  
326 1996;7:381-388.
- 327 5. Zhang Y, Li J, Xiao Y, et al. Genotype shift in human coronavirus OC43 and  
328 emergence of a novel genotype by natural recombination. *J Infect*. 2015;70:641-50.
- 329 6. Xiao Y, Rouzine IM, Bianco S, et al. RNA recombination enhances adaptability and is  
330 required for virus spread and virulence. *Cell Host Microbe*. 2017;22:420.
- 331 7. So RTY, Chu DKW, Miguel E, et al. Diversity of dromedary camel coronavirus  
332 HKU23 in African camels revealed multiple recombination events among closely  
333 related betacoronaviruses of the subgenus Embecovirus. *J Virol*. 2019;93:e01236-19.
- 334 8. Gribble J, Stevens LJ, Agostini ML, et al. The coronavirus proofreading  
335 exoribonuclease mediates extensive viral recombination. *PLoS Pathog*.  
336 2021;17(1):e1009226.
- 337 9. Bentley K, Evans DJ. Mechanisms and consequences of positive-strand RNA virus  
338 recombination. *J Gen Virol*. 2018;99:1345-1356.
- 339 10. Jackson B, Boni MF, Bull MJ, et al. Generation and transmission of interlineage  
340 recombinants in the SARS-CoV-2 pandemic. *Cell*. 2021;184:5179-5188.e8.



- 341 11. Francisco RDS Jr, Benites LF, Lamarca AP, et al. Pervasive transmission of E484K and  
342 emergence of VUI-NP13L with evidence of SARS-CoV-2 co-infection events by two  
343 different lineages in Rio Grande do Sul, Brazil. *Virus Res.* 2021;296:198345.
- 344 12. Taghizadeh P, Salehi S, Heshmati A, et al. Study on SARS-CoV-2 strains in Iran  
345 reveals potential contribution of co-infection with and recombination between different  
346 strains to the emergence of new strains. *Virology.* 2021;562:63-73.
- 347 13. Rockett, JD, Mailie G, Eby MS, et al. Co-infection with SARS-CoV-2 Omicron and  
348 Delta Variants revealed by genomic surveillance. *medRxiv* 2022; 2022.02.13.22270755;  
349 doi: <https://doi.org/10.1101/2022.02.13.22270755>.
- 350 14. Yi H. 2019 Novel coronavirus is undergoing active recombination. *Clin Infect Dis.*  
351 2020;71:884-887.
- 352 15. Yeh TY, Contreras GP. Emerging viral mutants in Australia suggest RNA  
353 recombination event in the SARS-CoV-2 genome. *Med J Aust.* 2020;213:44-44.e1.
- 354 16. VanInsberghe D, Neish AS, Lowen AC, Koelle K. Recombinant SARS-CoV-2  
355 genomes are currently circulating at low levels. *bioRxiv* 2021;2020.08.05.238386. doi:  
356 10.1101/2020.08.05.238386.
- 357 17. Gallaher WR. A palindromic RNA sequence as a common breakpoint contributor to  
358 copy-choice recombination in SARS-COV-2. *Arch Virol.* 2020;165:2341-2348.
- 359 18. Haddad D, John SE, Mohammad A, et al. SARS-CoV-2: Possible recombination and  
360 emergence of potentially more virulent strains. *PLoS One.* 2021;16:e0251368.
- 361 19. Makarenkov V, Mazoure B, Rabusseau G, Legendre P. Horizontal gene transfer and  
362 recombination analysis of SARS-CoV-2 genes helps discover its close relatives and  
363 shed light on its origin. *BMC Ecol Evol.* 2021;21:5.
- 364 20. Varabyou A, Pockrandt C, Salzberg SL, Pertea M. Rapid detection of inter-clade  
365 recombination in SARS-CoV-2 with Bolotie. *Genetics.* 2021;218:iyab074.

- 366 21. Leary S, Gaudieri S, Parker MD, et al. Generation of a novel SARS-CoV-2 sub-  
367 genomic RNA due to the R203K/G204R variant in nucleocapsid: homologous  
368 recombination has potential to change SARS-CoV-2 at both protein and RNA level.  
369 *Pathog Immun.* 2021;6:27-49.
- 370 22. Lohrasbi-Nejad A. Detection of homologous recombination events in SARS-CoV-2.  
371 *Biotechnol Lett.* 2022 Jan 17:1–16. doi: 10.1007/s10529-021-03218-7. Epub ahead of  
372 print.
- 373 23. Kreier F. Deltacron: the story of the variant that wasn't. *Nature.* 2022;602:19.
- 374 24. Ignatieva A, Hein J, Jenkins PA. Ongoing recombination in SARS-CoV-2 revealed  
375 through genealogical reconstruction. *Mol Biol Evol.* 2022;39:msac028.
- 376 25. Aksamentov I, Roemer C, Hodcroft EB, Neher RA. Nextclade: clade assignment,  
377 mutation calling and quality control for viral genomes. *Zenodo* 2021. doi:  
378 <https://doi.org/10.5281/zenodo.5607694>.
- 379 26. Hadfield J, Megill C, Bell SM, et al. Nextstrain: real-time tracking of pathogen  
380 evolution. *Bioinformatics.* 2018;34:4121-4123.
- 381 27. Rambaut A, Holmes EC, O'Toole Á, et al. A dynamic nomenclature proposal for SARS-  
382 CoV-2 lineages to assist genomic epidemiology. *Nat Microbiol.* 2020;5:1403-1407.
- 383 28. Colson P, Delerce J, Beye M, et al. First cases of infection with the 21L/BA.2 Omicron  
384 variant in Marseille, France. *medRxiv* 2022a; 2022.02.08.22270495; doi:  
385 <https://doi.org/10.1101/2022.02.08.22270495>.
- 386 29. Houhamdi L, Gautret P, Hoang VT, Fournier PE, Colson P, Raoult D. Characteristics of  
387 the first 1119 SARS-CoV-2 Omicron variant cases, in Marseille, France, November-  
388 December 2021. *J Med Virol.* 2022 Jan 20. doi: 10.1002/jmv.27613. Epub ahead of  
389 print.

- 390 30. Sayers EW, Cavanaugh M, Clark K, Pruitt KD, Schoch CL, Sherry ST, Karsch-  
391 Mizrachi I. GenBank. *Nucleic Acids Res.* 2022 Jan 7;50(D1):D161-D164.
- 392 31. Lole KS, Bollinger RC, Paranjape RS, Gadkari D, Kulkarni SS, Novak NG, Ingersoll R,  
393 Sheppard HW, Ray SC. Full-length human immunodeficiency virus type 1 genomes  
394 from subtype C-infected seroconverters in India, with evidence of intersubtype  
395 recombination. *J Virol.* 1999 Jan;73(1):152-60.
- 396 32. Nguyen LT, Schmidt HA, von Haeseler A, Minh BQ. IQ-TREE: a fast and effective  
397 stochastic algorithm for estimating maximum-likelihood phylogenies. *Mol Biol Evol.*  
398 2015 Jan;32(1):268-74. doi: 10.1093/molbev/msu300. Epub 2014 Nov 3. PMID:  
399 25371430; PMCID: PMC4271533.
- 400 33. Kumar S, Stecher G, Li M, Knyaz C, Tamura K. MEGA X: Molecular Evolutionary  
401 Genetics Analysis across Computing Platforms. *Mol Biol Evol.* 2018 Jun 1;35(6):1547-  
402 1549. doi: 10.1093/molbev/msy096. PMID: 29722887; PMCID: PMC5967553.
- 403 34. Katoh K, Misawa K, Kuma K, Miyata T. MAFFT: a novel method for rapid multiple  
404 sequence alignment based on fast Fourier transform. *Nucleic Acids Res.* 2002 Jul  
405 15;30(14):3059-66. doi: 10.1093/nar/gkf436. PMID: 12136088; PMCID: PMC135756.
- 406 35. Altschul SF, Gish W, Miller W, Myers EW, Lipman DJ. Basic local alignment search  
407 tool. *J Mol Biol.* 1990;215:403-10.
- 408 36. La Scola B, Le Bideau M, Andreani J, et al. Viral RNA load as determined by cell  
409 culture as a management tool for discharge of SARS-CoV-2 patients from infectious  
410 disease wards. *Eur J Clin Microbiol Infect Dis.* 2020;39:1059-1061.
- 411 37. Colson P, Lagier JC, Baudoin JP, Bou Khalil J, La Scola B, Raoult D. Ultrarapid  
412 diagnosis, microscope imaging, genome sequencing, and culture isolation of SARS-  
413 CoV-2. *Eur J Clin Microbiol Infect Dis.* 2020 Aug;39(8):1601-1603.

- 414 38. Fantini J, Yahi N, Azzaz F, Chahinian H. Structural dynamics of SARS-CoV-2 variants:  
415 A health monitoring strategy for anticipating Covid-19 outbreaks. *J Infect.*  
416 2021;83:197-206.
- 417 39. Fantini J, Yahi N, Colson P, Chahinian H, La Scola B, Raoult D. The puzzling  
418 mutational landscape of the SARS-2-variant Omicron. *J Med Virol.* 2022 Jan 8. doi:  
419 10.1002/jmv.27577. Epub ahead of print.
- 420 40. Bedotto M, Fournier PE, Houhamdi L, Colson P, Raoult D. Implementation of an in-  
421 house real-time reverse transcription-PCR assay to detect the emerging SARS-CoV-2  
422 N501Y variants. *J Clin Virol.* 2021;140:104868.
- 423 41. Raoult D. A viral grandfather: genomics in 2010 contradict Darwin's vision of  
424 evolution. *Eur J Clin Microbiol Infect Dis.* 2011;30:935-6.
- 425 42. Merhej V, Raoult D. Rhizome of life, catastrophes, sequence exchanges, gene creations,  
426 and giant viruses: how microbial genomics challenges Darwin. *Front Cell Infect*  
427 *Microbiol.* 2012;2:113.
- 428 43. Feschotte C, Gilbert C. Endogenous viruses: insights into viral evolution and impact on  
429 host biology. *Nat Rev Genet.* 2012;13:283-96.
- 430 44. Roux S, Enault F, Bronner G, Vaultot D, Forterre P, Krupovic M. Chimeric viruses blur  
431 the borders between the major groups of eukaryotic single-stranded DNA viruses. *Nat*  
432 *Commun.* 2013;4:2700.
- 433 45. Jacobs GS, Hudjashov G, Saag L, et al. Multiple deeply divergent Denisovan ancestries  
434 in Papuans. *Cell.* 2019;177:1010-1021.e32.
- 435 46. Liu X, Shao Y, Ma H, et al. Comparative analysis of four Massachusetts type infectious  
436 bronchitis coronavirus genomes reveals a novel Massachusetts type strain and evidence  
437 of natural recombination in the genome. *Infect Genet Evol.* 2013;14:29-38.

438 47. Hodcroft E. 2012. CoVariants: SARS-CoV-2 mutations and variants of interest.

439 Available from: <https://covariants.org/>.

440

441  
442  
443  
444  
445  
446  
447  
448  
449  
450  
451  
452  
453  
454  
455  
456  
457  
458  
459  
460  
461  
462  
463  
464  
465

## FIGURE LEGEND

**Figure 1. Schematic of the SARS-CoV-2 Delta 21J/AY.4-Omicron 21K/BA.1 recombinant genome, and phylogenetic trees based on different regions of the Deltamicron genome reflecting the origin of most of the viral genome from a Delta 21J/AY.4 variant and the origin of a region spanning a large part of the spike gene from a Omicron 21K/BA.1 variant.**

a: Map of the SARS-CoV-2 genome.

b: Schematic representation of parental and recombinant genomes.

c: Mutations in the three Delta 21J/AY.4-Omicron 21K/BA1 recombinant genomes. Adapted from screenshots of the nextclade web application output (<https://clades.nextstrain.org>).<sup>25,26</sup>

Color codes for nucleotide mutations and are marked regions as follows: Green: U; yellow: G; blue: C; red: A; grey: deletions or uncovered regions. Genomes are labelled with the identifiers of the IHU Méditerranée Infection and the GenBank (<https://www.ncbi.nlm.nih.gov/genbank/>)<sup>30</sup> sequence databases.

d, e: Phylogenetic trees based on different regions of the Deltamicron genomes showing the origin of most of the viral genome from a Delta 21J/AY.4 variant (d) and the origin of a region spanning a large part of the spike gene from a Omicron 21K/BA.1 variant (e). The 10 genomes the most similar genetically to these regions of the recombinant genomes obtained here were selected from the sequence database of our institute through a BLAST<sup>35</sup> search, then were incorporated in the phylogeny together with the genome of the Wuhan-Hu-1 isolate. Sequences are labelled with the identifiers of the IHU Méditerranée Infection and the GenBank (<https://www.ncbi.nlm.nih.gov/genbank/>)<sup>30</sup> sequence databases.

**Figure 2. Microscopy images of the virus cytopathic effect (a, b) and of a viral particle**

466 **(c) in culture of the SARS-CoV-2 Delta 21J/AY.4-Omicron 21K/BA.1 recombinant on**  
467 **Vero E6 cells.**

468 a. Absence of cytopathic effect (negative control: absence of virus); b. Cytopathic effect  
469 observed 4 days post-inoculation on Vero E6 cells of the respiratory sample of the first patient  
470 for whom the SARS-CoV-2 Delta 21J/AY.4-Omicron 21K/BA.1 recombinant was identified.  
471 c. Scanning electron microscopy image was obtained with a SU5000 microscope (Hitachi  
472 High-Technologies Corporation, Tokyo, Japan).

473

474 **Figure 3. Schematic of the predicted structure of the spike protein of the SARS-CoV-2**  
475 **Delta 21J/AY.4-Omicron 21K/BA.1 recombinant**

476 a. Overall structure of the recombinant spike protein. The secondary structure is in grey,  
477 mutated amino acids are in blue. NTD, N-terminal domain; RBD, receptor binding domain;  
478 S1-S2, cleavage site.

479 b. Superimposition of the secondary structure of the Omicron 21K/BA.1 variant (in cyan) and  
480 recombinant (in red) spike proteins. NTD, N-terminal domain; RBD, receptor binding  
481 domain.

482 c. Comparison of the electrostatic surface potential of the spike proteins in Delta 21J/AY.4  
483 lineage, Omicron 21K/BA.1 variant, and in the recombinant. The color scale (negative in red,  
484 positive in blue, neutral in white) is indicated. NTD, N-terminal domain; RBD, receptor  
485 binding domain.

486

487

488

**TABLE**

489  
490  
491

**Table 1. Nucleotide and amino acid changes in the Deltamicron recombinant according to their presence/absence in the Delta 21J/AY.4 lineage and the Omicron 21K/BA.1 variant.**

SARS-CoV-2 genes or genome regions	Nucleotide changes	Amino acid changes	Present in the Delta 21J/AY.4 lineage	Present in the Omicron 21K/BA.1 variant	Present in the Delta 21J/AY.4-Omicron 21K/BA.1 recombinant
5UTR	G210U	/	X		X
5UTR	C241U	/	X	X	X
ORF1a	A1321C	E352D			X
ORF1a	C3037U	/	X	X	X
ORF1a	G4181U	A1306S	X		X
ORF1a	C6402U	P2046L	X		X
ORF1a	C7124U	P2287S	X		X
ORF1a	C7851U	A2529V	X		X
ORF1a	A8723G	I2820V			X
ORF1a	C8986U	/	X		X
ORF1a	G9053U	V2930L	X		X
ORF1a	C10029U	T3255I	X	X	X
ORF1a	A11201G	T3646A	X		X
ORF1a	A11332G	/	X		X
ORF1b	C14407U	P314F / P314L			X
ORF1b	C14408U	P314F / P314L	X	X	X
ORF1b	U15264C	/	X		X
ORF1b	G15451A	G662S	X		X
ORF1b	C16466U	P1000L	X		X
ORF1b	C19220U	A1918V	X		X
S	C21618G	T19R	X		X
S	G21641U	A27S			X
S	C21846U	T95I	X	X	X
S	G21987A	G142D	X		X
S	GAGUUCA22028G	EFR156G	X		X
S	AAUU22193A	NL211I		X	X
S	U22204UGAGCCAGAA	Ins214EPE		X	X
S	G22578A	G339D		X	X
S	UC22673CU	S371L		X	X
S	U22679C	S373P		X	X
S	C22686U	S375F		X	X
S	G22813U	K417N		X	X
S	U22882G	N440K		X	X
S	G22898A	G446S		X	X
S	G22992A	S477N		X	X
S	C22995A	T478K	X	X	X
S	A23013C	E484A		X	X
S	A23040G	Q493R		X	X
S	G23048A	G496S		X	X
S	A23055G	Q498R		X	X
S	A23063U	N501Y		X	X
S	U23075C	Y505H		X	X
S	C23202A	T547K		X	X
S	A23403G	D614G	X	X	X
S	C23525U	H655Y		X	X
S	U23599G	N679K		X	X
S	C23604A	P681H		X	X
S	C23854A	N764K		X	X
S	G23948U	D796Y		X	X
S	C24130A	N856K		X	X
S	A24424U	Q954H		X	X
S	U24469A	N969K		X	X
S	C24503U	L981F		X	X
S	C25000U	/		X	X
ORF3a	C25667U	S92L			X
ORF3a	G25855U	D155Y			X
M	U26767C	I82T	X		X
ORF7a	U27638C	V82A	X		X
ORF7a	C27752U	T120I	X		X
ORF7b	C27874U	T40I	X		X
ORF8	AGAUUUC28247A	DF119Del	X		X
Intergenic region	UA28270U	/	X		X
N	A28461G	D63G	X		X
N	G28881U	R203M	X		X
N	G28916U	G215C	X		X
N	G29402U	D377Y	X		X
Intergenic region	G29540A	/			X
ORF10	G29645U	/			X
3UTR	G29742U	/	X		X

492  
493

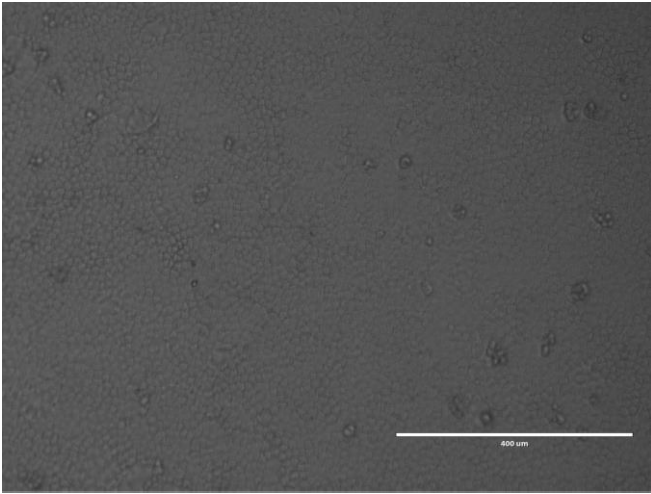
/, no change; Ins, insertion; Del, deletion; UTR, untranslated region; X, present. S gene region is indicated by a grey background.



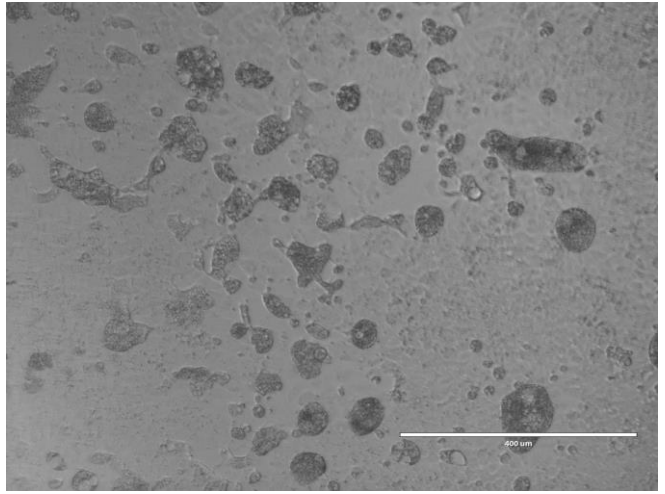


**Fig. 2**

**a.**



**b.**



**c.**

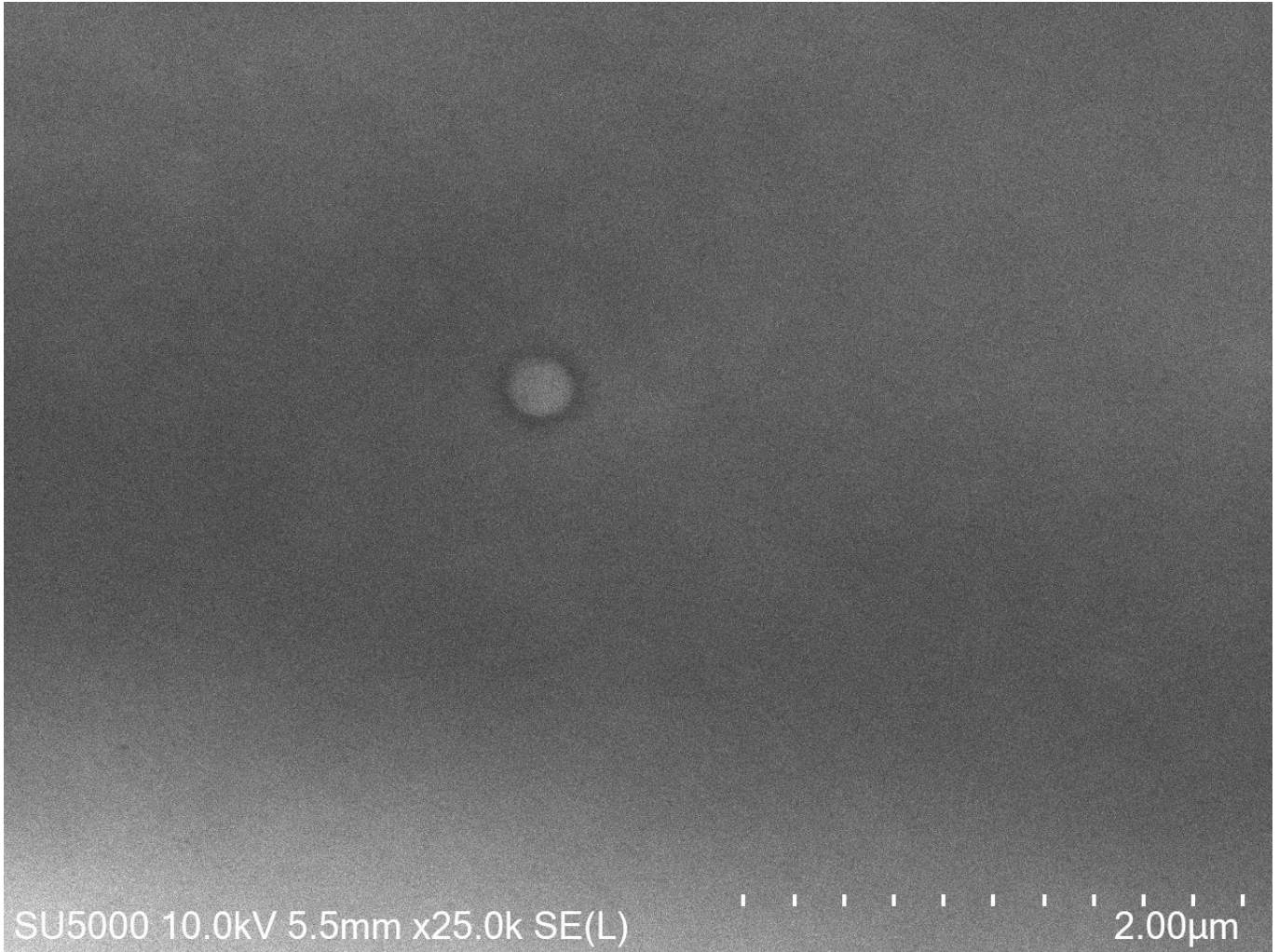


Fig. 3

